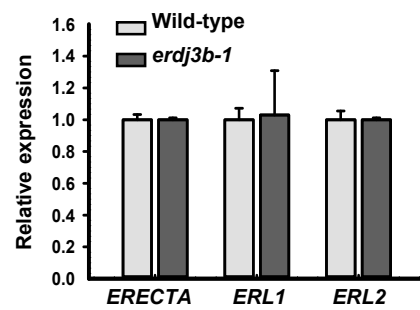
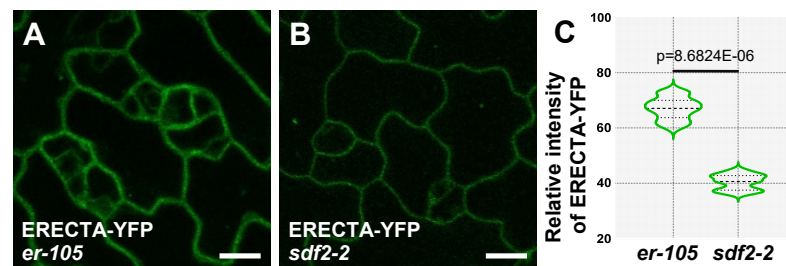


**Fig. S1. Endo-H assay of ERECTA-family proteins and ERL2-YFP expression after TM treatment.**

(A-C) RT-qPCR analysis of the transcript levels of ERECTA-family genes. No significant differences are found between mock (DMSO) and TM treatments. Data are mean $\pm$ s.d. of three biological replicates. (D) Immunoblotting analysis of ERECTA-FLAG extracted from mock and TM-treated plants with and without Endo-H digestion. ERECTA-FLAG from TM-treated plants was sensitive to Endo-H digestion, showing a stronger lower band (cleaved proteins) in immunoblot after Endo-H digestion (pink arrowhead). Prolonged Endo-H digestion of 40 min or 60 min produced two bands in control plants. While, the upper band (non-cleaved proteins) was faint in TM-treated plants (blue arrowhead). The samples without Endo-H digestion are presented as control (left two lanes). Notice the fast moving of ERECTA-FLAG protein from the TM-treated plants. (E) Immunoblotting analysis of ERL1-FLAG protein after Endo-H digestion. ERL1-FLAG from TM-treated plants was sensitive to Endo-H digestion, showing a faster mobility in immunoblot. (F, G) Confocal images of *ERL2:ERL2-YFP* epidermis. Strong intracellular ERL2-YFP signals were detected in the stomatal precursor cells after TM treatment. (H) Immunoblotting analysis of ERL2-FLAG with and without Endo-H digestion. In contrast to the two bands of ERL2-FLAG in control plants (blue and pink arrowheads), Endo-H digestion of ERL2-FLAG protein from TM-treated plants resulted in a single band with faster mobility. Lower panel, the loading control of actin detected by anti-Actin (green arrowhead). (I-N) Immunoblotting analysis of ERECTA-FLAG, ERL1-FLAG and ERL2-FLAG extracted from mock and treated with TM, CHX, TM with CHX, MG-132, and TM with MG-132. Top panel, the ERECTA-family protein bands detected by anti-FLAG (red arrowhead). Lower panel, the loading control of actin detected by anti-Actin (green arrowhead). The red numbers above the upper panel are relative ratios of mean gray values of bands to the DMSO control. (O-R) No obvious changes of SERK3-YFP and BRI1-GFP in epidermis were observed after TM treatment. Images are representative of three independent experiments. Scale bars: 20  $\mu$ m.



**Fig. S2. RT-qPCR analysis of the transcript levels of ERECTA-family genes.** No significant differences were found between wild-type and *erdj3b-1* mutant. Data are mean $\pm$ s.d. of three biological replicates.



**Fig. S3. The overall fluorescence intensity of ERECTA-YFP is reduced in *sdf2-2* mutant.** (A, B) Confocal images of ERECTA-YFP in *er-105* (complementary) and *sdf2-2* mutant leaf epidermis. Scale bars: 20  $\mu$ m. (C) Quantification fluorescence intensity in stomatal precursor cells. ERECTA-YFP intensity in *er-105* is statistically different from that in *sdf2-2* after two-tailed unpaired Student's *t*-test ( $n=21$ ). Dotted lines indicate the 25th-75th percentiles and dashed lines indicate the median.

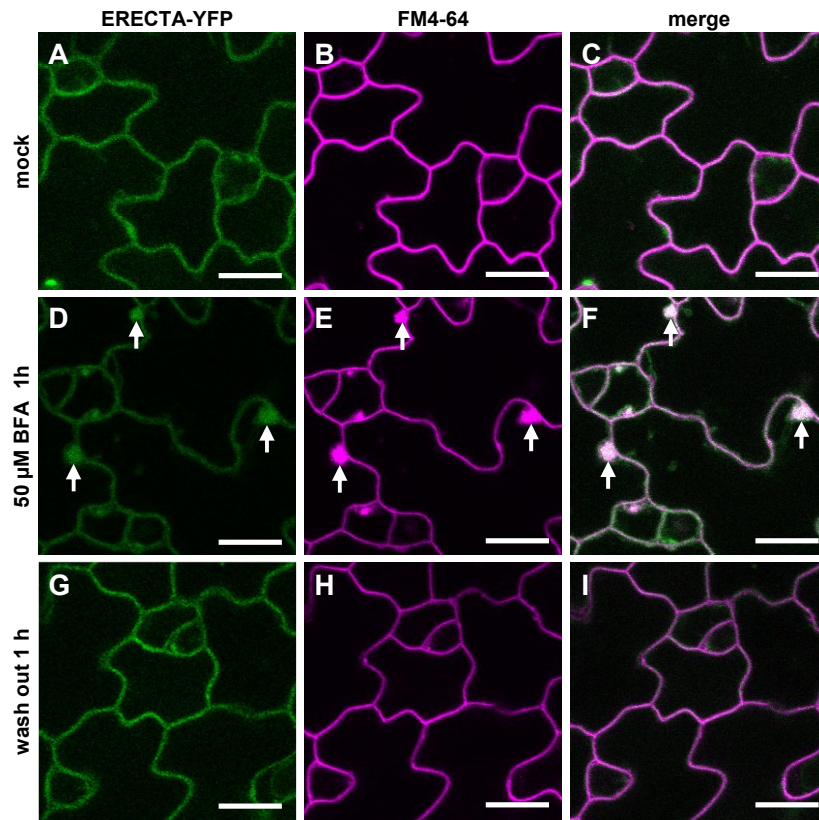


**Fig. S4. Effects of BFA on subcellular localization of ERECTA-YFP.**

(A-C) Confocal images show the colocalization of ERECTA-YFP (*er-105* complementary) with FM4-64 at the PM. (D-F) Confocal images show the aggregation of ERECTA-YFP and FM4-64 in BFA-bodies (white arrows) at 1 h after 50 μM BFA treatment. (G-I) Confocal images show the colocalization of ERECTA-YFP colocalizes with FM4-64 at the PM in BFA-treated plants after 1 h water rinse (wash out).

Scale bars: 20 μm.

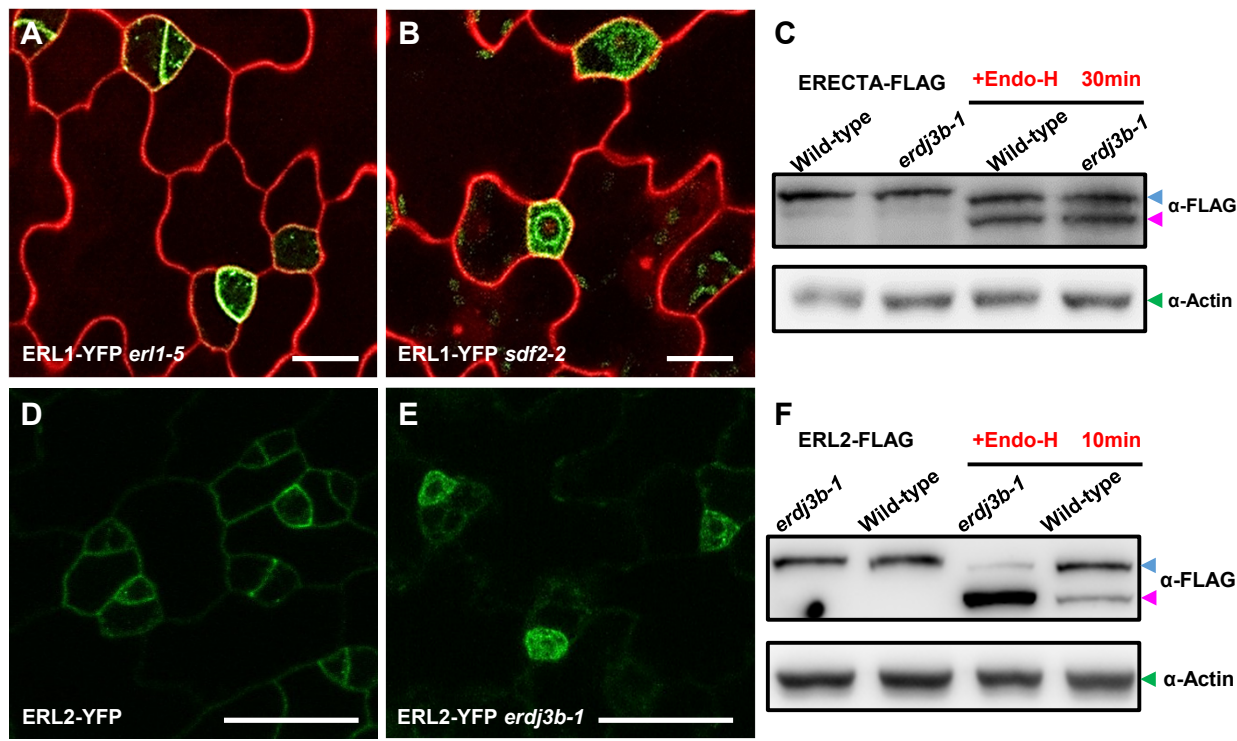


**Fig. S5. Dysfunction of SDF2-ERdj3B-BiP complex causes retention of ERL1 and ERL2 in the ER.**

(A, B) ERL1-YFP (*erl1-5* complementary) predominantly localizes at the PM in stomatal precursor cells. In *sdf2-2*, ERL1-YFP is present in ring-like structure. Cell outlines are visualized with propidium iodide. (C) Immunoblot analysis of ERECTA-FLAG after Endo-H digestion. ERECTA-FLAG proteins extracted from wild-type and *erdj3b-1* plants show a similar response to Endo-H digestion. A blue and a pink arrowhead indicate the non-cleaved proteins (upper band) and cleaved proteins (lower band), respectively. Lower panel, loading control of actin detected by anti-Actin. (D, E) ERL2-YFP predominantly resides at the PM of stomatal precursor cells in the wild-type plants. In *erdj3b-1*, strong ERL2-YFP signals are detected in the ring-like structure. (F) Immunoblot analysis of ERL2 after Endo-H digestion. ERL2-FLAG protein extracted from *erdj3b-1* plants are sensitive to Endo-H digestion, comparing with ERL2-FLAG in wild-type plants, showing a stronger lower band (cleaved proteins) in immunoblot analysis. Images are representative of three independent experiments.

Scale bars: 20 μm.

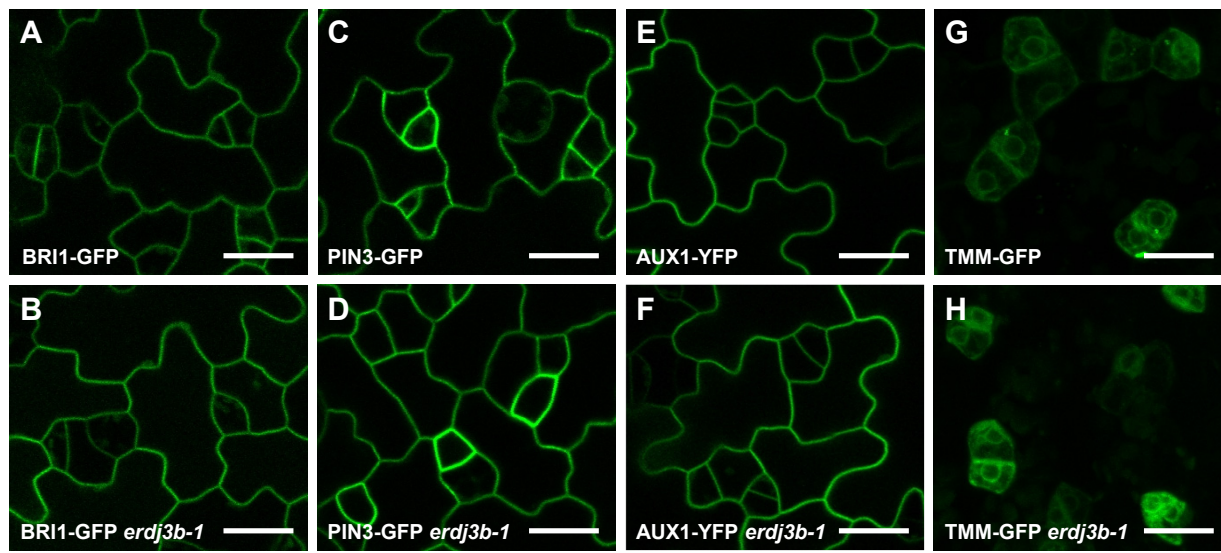


**Fig. S6. BRI1-GFP, PIN3-GFP, AUX1-YFP and TMM-GFP expression in wild-type and *erdj3b-1* epidermis.**

No obvious changes of BRI1-GFP, PIN3-GFP, AUX1-YFP, and TMM-GFP expression and localization were found in *erdj3b-1* mutant epidermis, comparing that in wild-type background.

Scale bars: 20  $\mu$ m.

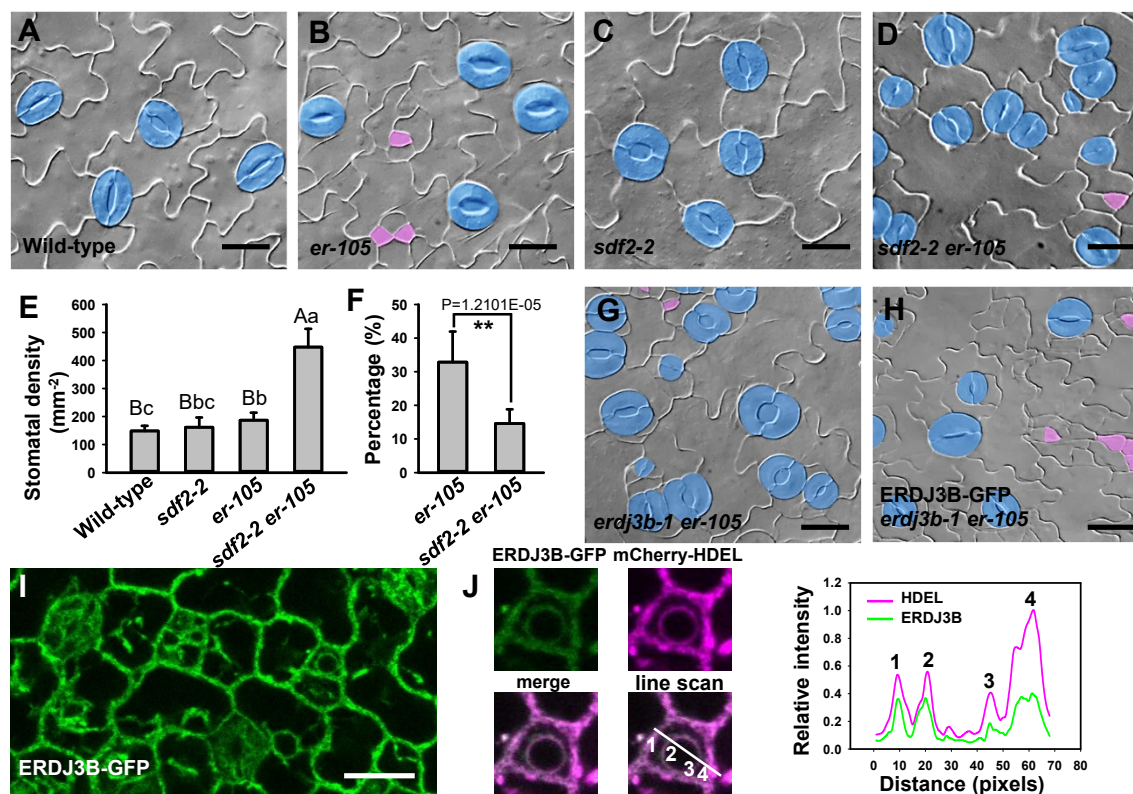


### Fig. S7. ER-resident SDF2-ERdj3B-BiP is differentially involved in stomatal development regulation.

(A-D) DIC images of epidermis of 12-day-old cotyledons. Mature stomata are highlighted by blue color. Precursor-like Cells (PrCs) are highlighted by pink color. Mutation of *sdf2* promotes the differentiation of PrCs in *er-105* into mature stomata, leading to an increase of stomatal production and stomatal clusters. (E) Quantitative analysis of stomatal density. Values are mean $\pm$ s.d. ( $n=18$ ). Data were analyzed using one-way ANOVA with Tukey's post hoc test. The different uppercase and lowercase letters indicate significant differences at 1% and 5%, respectively. (F) Quantification of the percentage of PrCs over total number of PrCs and mature stomata. Values are mean $\pm$ s.d.. Asterisks indicate significant difference after two-tailed unpaired Student's *t*-test,  $**P<0.01$ . (G, H) Introduction of *ERDJ3B:ERDJ3B-GFP* restored the appearance of arrested precursor cells in *erdj3b-1 er-105*, resembling the stomatal phenotype in *er-105* single mutant. (I) Confocal image of *ERDJ3B:ERDJ3B-GFP* expression in epidermis cells. (J) Quantitative analysis of fluorescence intensity profiles revealed the colocalization of ERDJ3B-GFP with mCherry-HDEL in the ER. Scale bars: 20  $\mu$ m.

### Table S1. Nucleotide sequences of primer sets used in this study.

[Click here to download Table S1](#)